

# Data Science, Time Complexity & Spacekime Analytics

Ivo D. Dinov

## Statistics Online Computational Resource

Health Behavior & Biological Sciences  
Computational Medicine & Bioinformatics  
Neuroscience Graduate Program  
Michigan Institute for Data Science  
University of Michigan

<http://SOCR.umich.edu>



Joint work with Milen V. Velev (BTU)

Based on an upcoming book "*Data Science: Time Complexity and Inferential Uncertainty*"



SCHOOL OF NURSING

STATISTICS ONLINE COMPUTATIONAL RESOURCE (SOCR)  
UNIVERSITY OF MICHIGAN

Slides Online:  
"SOCR News"

## Outline

- ☐ Motivation: Big Data Analytics Challenges
- ☐ Complex-Time (*kime*)
- ☐ Spacekime Calculus & Math Foundations
- ☐ Open Spacekime Problems
- ☐ Statistical Implications of Spacekime Analytics
  - ☐ Bayesian Inference Representation
- ☐ Applications – Longitudinal Spacekime Data Analytics
  - ☐ Neuroimaging (UKBB, fMRI)
  - ☐ Air quality (UCI ML Air Quality Dataset )



# Big Data Analytics Challenges



## Data Analytics = Information Compression

- ❑ From 23 ... to ...  $2^{23}$  (10M)  $\left( \underbrace{23}_{2 \text{ #'s}} \rightarrow \underbrace{2^{23}}_{8 \text{ #'s}} \right)$
- ❑ Two centuries of Data Science: 1798  $\rightarrow$  2020
- ❑ In the 18<sup>th</sup> century, Henry Cavendish used just 23 observations to answer a fundamental question – “What is the Mass of the Earth?” He estimated very accurately the mean density of the Earth/H<sub>2</sub>O ( $5.483 \pm 0.1904 \text{ g/cm}^3$ )
- ❑ In the 21<sup>st</sup> century to achieve the same scientific impact, matching the reliability and the precision of the Cavendish’s 18<sup>th</sup> century prediction, requires a monumental community effort using massive and complex information often exceeding 10M ( $2^{23}$ ) bytes



# Common Characteristics of Big Data

IBM Big Data 4V's: Volume, Variety, Velocity & Veracity

Big Bio Data Dimensions	Tools
<b>Size</b>	Harvesting and management of vast amounts of data
<b>Complexity</b>	Wranglers for dealing with heterogeneous data
<b>Incongruency</b>	Tools for data harmonization and aggregation
<b>Multi-source</b>	Transfer and joint multivariate representation & modeling
<b>Multi-scale</b>	Macro $\rightarrow$ meso $\rightarrow$ micro $\rightarrow$ nano scale observations
<b>Time</b>	Techniques accounting for longitudinal effects (e.g., time corr)
<b>Incomplete</b>	Reliable management of missing data, imputation

**Example:** analyzing observational data of 1,000's Parkinson's disease patients based on 10,000's signature biomarkers derived from multi-source imaging, genetics, clinical, physiologic, phenomics and demographic data elements

Software developments, student training, service platforms and methodological advances associated with the Big Data Discovery Science all present existing opportunities for learners, educators, researchers, practitioners and policy makers

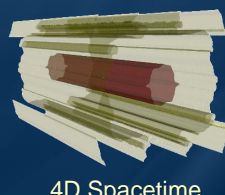
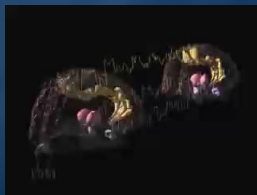
Dinov, *GigaScience* (2016) PMID:26918190



## Longitudinal Data Analytics

### □ Neuroimaging:

- **4D fMRI:** time-series, represents measurements of hydrogen atom densities over a 3D lattice of spatial locations ( $1 \leq x, y, z \leq 64$  pixels), about  $3 \times 3$  millimeters<sup>2</sup> resolution. Data is recorded longitudinally over time ( $1 \leq t \leq 180$ ) in increments of about 3 seconds, then post-processed
- **State-of-the-art Approaches:** Time-series modeling or Network analysis
- **Spacekime Analytics:** 5D fMRI kime-series, represent the hydrogen atom densities over the same 3D lattice of spatial locations, longitudinally over the 2D kime space,  $\kappa = re^{i\phi} \in \mathbb{C}$
- **Differences:** Spacekime analytics estimate and utilize the kime-phases



4D Spacetime

4D/5D Reconstructions



5D Spacekime

Dinov & Velez (2021)

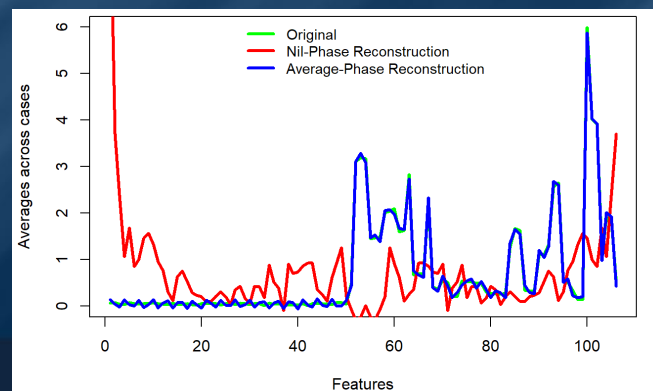


# Complex-Time (*kime*) & Spacekime Foundations



## Example of a Driving Biomed Problem

- Preview: Before we get to Big Data Analytics, we need some background
- Complex Problem: 10,000 UKBB participants; 7,614 clinical measurements, phenotypic features, and derived neuroimaging biomarkers. Supervised Decision Tree (binary) Classification; clinical outcome = mental health



# The Fourier Transform

By separability, the classical **spacetime Fourier transform** is just four Fourier transforms, one for each of the four spacetime dimensions,  $(\mathbf{x}, t) = (x, y, z, t)$ . The FT is a function of the angular frequency  $\omega$  that propagates in the wave number direction  $\mathbf{k}$  (space frequency). Symbolically, the forward and inverse Fourier transforms of a 4D ( $n = 4$ ) spacetime function  $f$ , are defined by:

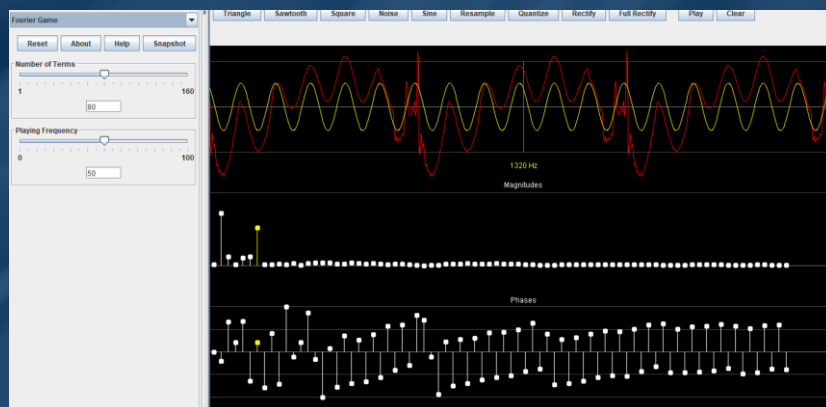
$$FT(f) = \hat{f}(\mathbf{k}, \omega) = \frac{1}{(2\pi)^{\frac{n}{2}}} \int f(\mathbf{x}, t) e^{i(\omega t - \mathbf{k}\mathbf{x})} dt d^3\mathbf{x},$$

$$IFT(\hat{f}) = \hat{\hat{f}}(\mathbf{x}, t) = \frac{1}{(2\pi)^{\frac{n}{2}}} \int \hat{f}(\mathbf{k}, \omega) e^{-i(\omega t - \mathbf{k}\mathbf{x})} d\omega d^3\mathbf{k}.$$

$$\left[ \hat{\hat{f}}(\mathbf{x}, t) = IFT(\hat{f}) = IFT(FT(f)) = f(\mathbf{x}, t), \quad \forall \mathbf{z} \in \mathbb{C}, z = \underbrace{A}_{mag} e^{i \underbrace{\varphi}_{phase}} \right]$$



## 1D Fourier Transform Example



**SOCR 1D Fourier / Wavelet signal decomposition into *magnitudes* and *phases* (Java applet)**

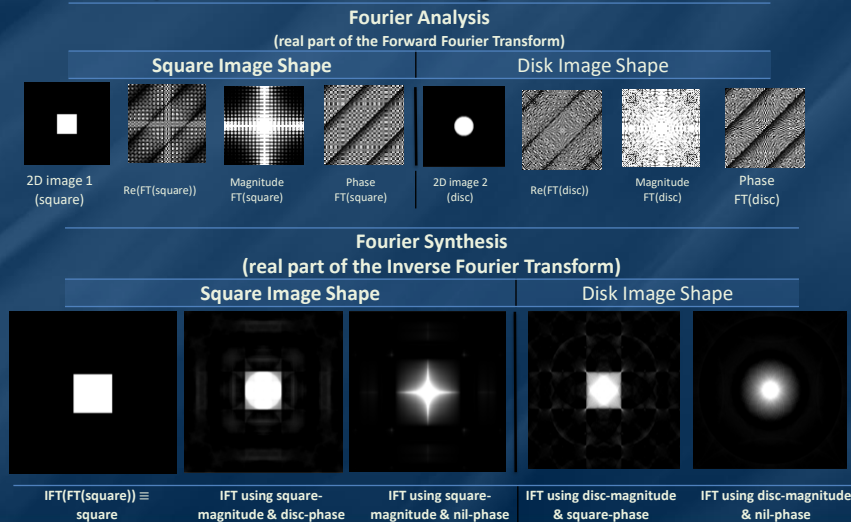
**Top-panel:** original signal (image), white-color curve drawn manually by the user and the reconstructed synthesized (IFT) signal, red-color curve, computed using the user modified magnitudes and phases

**Bottom-panels:** the Fourier analyzed signal (FT) with its magnitudes and phases

[http://www.socr.ucla.edu/htmls/game/Fourier\\_Game.html](http://www.socr.ucla.edu/htmls/game/Fourier_Game.html) (Java Applet)

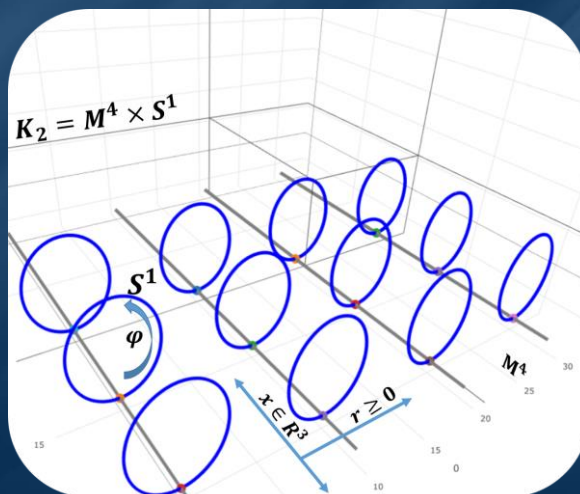


## 2D Fourier Transform – The Importance of Magnitudes & Phases



## Kaluza-Klein Theory

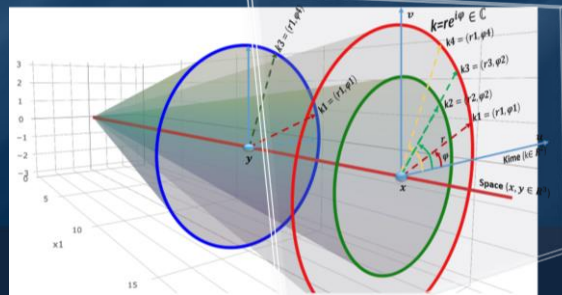
- Theodor Kaluza developed (1921) an extension of the classical general relativity theory to 5D. This included the metric, the field equations, the equations of motion, the stress-energy tensor, and the cylinder condition. Oskar Klein (1926) interpreted Kaluza's 3D+2D theory in quantum mechanical space and proposed that the fifth dimension was curled up and microscopic.
- The topology of the 5D Kaluza-Klein spacetime is  $K_2 \cong M^4 \times S^1$ , where  $M^4$  is a 4D Minkowski spacetime and  $S^1$  is a circle (non-traversable).



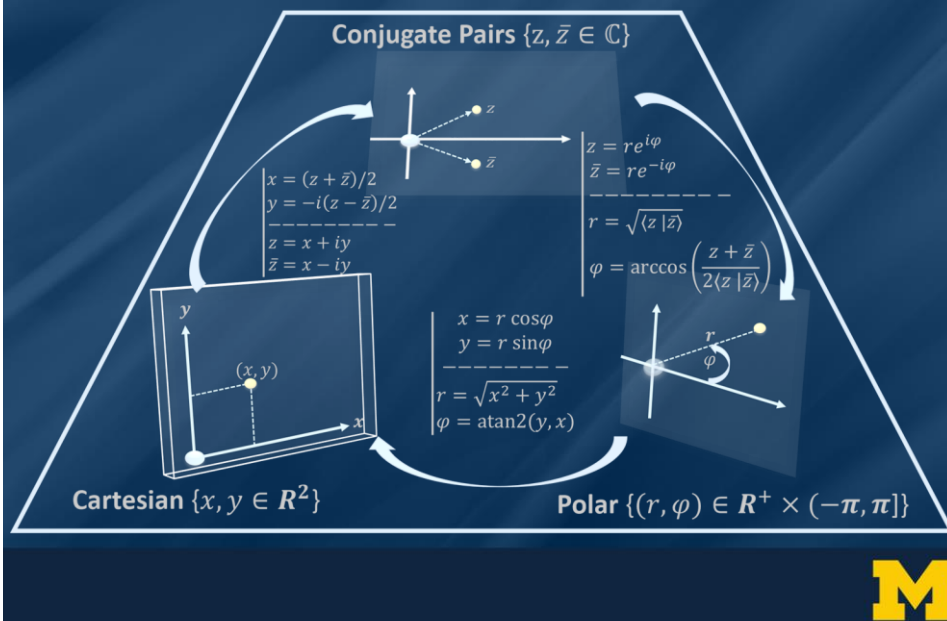


## Complex-Time (Kime)

- At a given spatial location,  $x$ , complex time (kime) is defined by  $\kappa = re^{i\varphi} \in \mathbb{C}$ , where:
  - the magnitude represents the longitudinal events order ( $r > 0$ ) and characterizes the longitudinal displacement in time, and
  - event phase ( $-\pi \leq \varphi < \pi$ ) is an angular displacement, or event direction
- There are multiple alternative parametrizations of kime in the complex plane
- Space-kime manifold is  $R^3 \times \mathbb{C}$ :
  - $(x, k1)$  and  $(x, k4)$  have the same spacetime representation, but different spacekime coordinates,
  - $(x, k1)$  and  $(y, k1)$  share the same kime, but represent different spatial locations,
  - $(x, k2)$  and  $(x, k3)$  have the same spatial-locations and kime-directions, but appear sequentially in order



## Kime Parameterizations



# The Spacetime Manifold

- **Spacetime:**  $(x, k) = \left( \underbrace{x^1, x^2, x^3}_{\text{space}}, \underbrace{ck_1 = x^4, ck_2 = x^5}_{\text{kime}} \right) \in X, \quad c \sim 3 \times 10^8 \text{ m/s}$
- **Kevents** (*complex events*): points (or states) in the spacetime manifold  $X$ . Each kevent is defined by where  $(x = (x, y, z))$  it occurs in space, what is its *causal longitudinal order*  $(r = \sqrt{(x^4)^2 + (x^5)^2})$ , and in what *kime-direction*  $(\varphi = \text{atan2}(x^5, x^4))$  it takes place.
- **Spacetime interval** ( $ds$ ) is defined using the general Minkowski  $5 \times 5$  metric tensor  $(\lambda_{ij})_{i=1, j=1}^{5,5}$ , which characterizes the geometry of the (*generally curved*) spacetime manifold:
 
$$ds^2 = \sum_{i=1}^5 \sum_{j=1}^5 \lambda_{ij} dx^i dx^j = \lambda_{ij} dx^i dx^j$$

$$(\lambda_{ij}) = \begin{bmatrix} 1 & 0 & 0 & 0 & 0 \\ 0 & 1 & 0 & 0 & 0 \\ 0 & 0 & 1 & 0 & 0 \\ 0 & 0 & 0 & -1 & 0 \\ 0 & 0 & 0 & 0 & -1 \end{bmatrix}$$
- **Euclidean (flat) spacetime** metric corresponds to the tensor:
  - **Spacelike** intervals correspond to  $ds^2 > 0$ , where an inertial frame can be found such that two kevents  $a, b \in X$  are simultaneous. An object can't be present at two kevents which are separated by a spacelike interval.
  - **Lightlike** intervals correspond to  $ds^2 = 0$ . If two kevents are on the line of a photon, then they are separated by a lightlike interval and a ray of light could travel between the two kevents.
  - **Timelike** intervals correspond to  $ds^2 < 0$ . An object can be present at two different kevents, which are separated by a timelike interval.



# Spacetime Calculus

- Kime **Wirtinger derivative** (first order kime-derivative at  $k = (r, \varphi)$ ):
 
$$f'(z) = \frac{\partial f(z)}{\partial z} = \frac{1}{2} \left( \frac{\partial f}{\partial x} - i \frac{\partial f}{\partial y} \right) \quad \text{and} \quad f'(\bar{z}) = \frac{\partial f(\bar{z})}{\partial \bar{z}} = \frac{1}{2} \left( \frac{\partial f}{\partial x} + i \frac{\partial f}{\partial y} \right).$$

In Conjugate-pair basis:  $df = \partial f + \bar{\partial} f = \frac{\partial f}{\partial z} dz + \frac{\partial f}{\partial \bar{z}} d\bar{z}$

In Polar kime coordinates:

$$f'(k) = \frac{\partial f(k)}{\partial k} = \frac{1}{2} \left( \cos \varphi \frac{\partial f}{\partial r} - r \sin \varphi \frac{\partial f}{\partial \varphi} - i \left( \sin \varphi \frac{\partial f}{\partial r} + \frac{1}{r} \cos \varphi \frac{\partial f}{\partial \varphi} \right) \right)$$

$$f'(\bar{k}) = \frac{\partial f(\bar{k})}{\partial \bar{k}} = \frac{1}{2} \left( \cos \varphi \frac{\partial f}{\partial r} - r \sin \varphi \frac{\partial f}{\partial \varphi} + i \left( \sin \varphi \frac{\partial f}{\partial r} + \frac{1}{r} \cos \varphi \frac{\partial f}{\partial \varphi} \right) \right).$$
- Kime **Wirtinger acceleration** (second order kime-derivative at  $k = (r, \varphi)$ ):
 
$$f''(k) = \frac{1}{4r^2} \left( (\cos \varphi - i \sin \varphi)^2 \left( 2i \frac{\partial f}{\partial \varphi} - \frac{\partial^2 f}{\partial \varphi^2} + r \left( -\frac{\partial f}{\partial r} - 2i \frac{\partial^2 f}{\partial r \partial \varphi} + r \frac{\partial^2 f}{\partial r^2} \right) \right) \right).$$





# Spacekime Calculus

## □ Kime Wirtinger integration:

The *path-integral* of a complex function  $f: \mathbb{C} \rightarrow \mathbb{C}$  on a specific path connecting  $z_a \in \mathbb{C}$  to  $z_b \in \mathbb{C}$  is defined by generalizing Riemann sums:

$$\lim_{|z_{i+1}-z_i| \rightarrow 0} \sum_{i=1}^{n-1} (f(z_i)(z_{i+1} - z_i)) \cong \oint_{z_a}^{z_b} f(z_i) dz.$$

This assumes the path is a polygonal arc joining  $z_a$  to  $z_b$ , via  $z_1 = z_a, z_2, z_3, \dots, z_n = z_b$ , and we integrate the piecewise constant function  $f(z_i)$  on the arc joining  $z_i \rightarrow z_{i+1}$ .

*Assumptions*: the path  $z_a \rightarrow z_b$  needs to be defined and the limit of the generalized Riemann sums, as  $n \rightarrow \infty$ , will yield a complex number representing the Wirtinger integral of the function over the path.

## □ Similarly, extend the classical area integrals, indefinite integral, and Laplacian:

*Definite area integral*: for  $\Omega \subseteq \mathbb{C}$ ,  $\int_{\Omega} f(z) dz d\bar{z}$ .

*Indefinite integral*:  $\int f(z) dz d\bar{z}$ ,  $df = \frac{\partial f}{\partial z} dz + \frac{\partial f}{\partial \bar{z}} d\bar{z}$ .

The *Laplacian* in terms of conjugate pair coordinates is  $\Delta f = d^2 f = 4 \frac{\partial f}{\partial z} \frac{\partial f}{\partial \bar{z}} = 4 \frac{\partial f}{\partial \bar{z}} \frac{\partial f}{\partial z}$ .

Dinov & Velev (2021)



# Newton's equations of motion in kime

$$\left| \begin{array}{l} v = at + v_o \\ x = x_o + v_o t + \frac{1}{2} at^2 \\ v^2 = 2ax + v_o^2 \end{array} \right| \Rightarrow \left| \begin{array}{l} v = a_1 k_1 + v_{o1} = a_2 k_2 + v_{o2} \\ x = x_{o1} + v_{o1} k_1 + \frac{1}{2} a_1 k_1^2 = x_{o2} + v_{o2} k_2 + \frac{1}{2} a_2 k_2^2 \\ v v_1 = 2a_1 x + v_{o1}^2 \\ v v_2 = 2a_2 x + v_{o2}^2 \end{array} \right|$$

## □ Derived from the Kime Wirtinger velocity and acceleration

□ Kime-velocity ( $k = (t, \varphi)$ ) is defined by the Wirtinger derivative of the position with respect to kime:

$$v(k) = \frac{\partial x}{\partial k} = \frac{1}{2} \left( \cos \varphi \frac{\partial x}{\partial t} - \frac{1}{t} \sin \varphi \frac{\partial x}{\partial \varphi} - i \left( \sin \varphi \frac{\partial x}{\partial t} + \frac{1}{t} \cos \varphi \frac{\partial x}{\partial \varphi} \right) \right)$$

□ The directional kime derivatives  $v_1$  and  $v_2$ :

$$v_1 = \frac{\sqrt{dx^2 + dy^2 + dz^2}}{dk_1} = \frac{\sqrt{dx^2 + dy^2 + dz^2}}{\cos(\varphi) dt - t \sin(\varphi) d\varphi}, \quad v_2 = \frac{\sqrt{dx^2 + dy^2 + dz^2}}{dk_2} = \frac{\sqrt{dx^2 + dy^2 + dz^2}}{\sin(\varphi) dt + t \cos(\varphi) d\varphi}.$$

□ Equ.1: As  $a_1 = \frac{\partial v}{\partial k_1}$  and  $a_2 = \frac{\partial v}{\partial k_2}$ , integrating both sides yields  $\int a_1 dk_1 = \int dv$  and  $\int a_2 dk_2 = \int dv$ . Since the acceleration is constant in kime,  $v = a_1 \int dk_1 = a_1 k_1 + v_{o1} = a_2 \int dk_2 = a_2 k_2 + v_{o2}$ , where  $v_{o1}$  and  $v_{o2}$  are constants representing the initial k-velocities, defined in relation to the kime dimensions  $k_1$  and  $k_2$ , respectively.

□ Equ.2:  $v = \frac{\partial f_1}{\partial k_1} = a_1 k_1 + v_{o1}$  and  $v = \frac{\partial f_2}{\partial k_2} = a_2 k_2 + v_{o2}$  (from equ 1), integrating we get  $\int \partial f_1 = \int a_1 k_1 \partial k_1 + v_{o1} \int \partial k_1$  and  $\int \partial f_2 = \int a_2 k_2 \partial k_2 + v_{o2} \int \partial k_2$ . As  $a_1$  and  $a_2$  are constants, we have  $x = a_1 \int \partial \frac{k_1^2}{2} + v_{o1} k_1 = a_1 \frac{k_1^2}{2} + v_{o1} k_1 + C_1$  and we can compute the constant  $C_1 = x_{o1}$  by setting  $k_1 = 0$ . Analogously, we will have  $x = a_2 \int \partial \frac{k_2^2}{2} + v_{o2} k_2 = a_2 \frac{k_2^2}{2} + v_{o2} k_2 + C_2$ , and we estimate the constant  $C_2 = x_{o2}$  by setting  $k_2 = 0$ .

□ Equ.3:  $a_1 = \frac{\partial v}{\partial k_1} = \frac{\partial v}{\partial t} \times \frac{\partial t}{\partial k_1} = \frac{\partial v}{\partial t} \times v_1 = v_1 \frac{\partial v}{\partial x}$ . Again integrating, we get  $\int a_1 dx = \int v_1 dv = \int \frac{v}{\cos(\varphi)} dv = \frac{1}{\cos(\varphi)} \int v dv$  and thus,  $a_1 x + C_1 = \frac{v^2}{2 \cos(\varphi)}$ . Under the initial condition ( $v_o = v(0)$ ) this becomes  $2a_1 x + v_{o1}^2 = vv_1$ .

□ Equ.4: Analogously, we will have  $2a_2 x + v_{o2}^2 = vv_2$ .

Dinov & Velev (2021)



## Spacekime Generalizations

- Spacekime generalization of Lorentz transform between two reference frames,  $K$  &  $K'$ :

(the interval  $ds$  is Lorentz transform invariant)

$$\underbrace{\begin{pmatrix} x' \\ y' \\ z' \\ k'_1 \\ k'_2 \end{pmatrix}}_{\in K'} = \begin{pmatrix} \zeta & 0 & 0 & -\frac{c^2}{v_1}\beta^2\zeta & -\frac{c^2}{v_2}\beta^2\zeta \\ 0 & 1 & 0 & 0 & 0 \\ 0 & 0 & 1 & 0 & 0 \\ -\frac{1}{v_1}\beta^2\zeta & 0 & 0 & 1 + (\zeta - 1)\frac{c^2}{(v_1)^2}\beta^2 & (\zeta - 1)\frac{c^2}{v_1 v_2}\beta^2 \\ -\frac{1}{v_2}\beta^2\zeta & 0 & 0 & (\zeta - 1)\frac{c^2}{v_1 v_2}\beta^2 & 1 + (\zeta - 1)\frac{c^2}{(v_2)^2}\beta^2 \end{pmatrix} \underbrace{\begin{pmatrix} x \\ y \\ z \\ k_1 \\ k_2 \end{pmatrix}}_{\in K}$$

$$\text{where } 0 \leq \beta = \frac{1}{\sqrt{\left(\frac{c}{v_1}\right)^2 + \left(\frac{c}{v_2}\right)^2}} \leq 1 \quad \& \quad \zeta = \frac{1}{\sqrt{1 - \beta^2}} \geq 1.$$

Dinov & Velez (2021)



## Spacekime Math Generalizations

- Derived other spacekime concepts: law of addition of velocities, energy-momentum conservation law, stability conditions for particles moving in spacekime, conditions for nonzero rest particle mass, and causal structure of spacekime ...

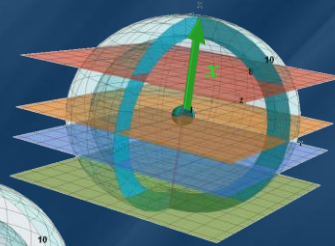
Dinov & Velez (2021)



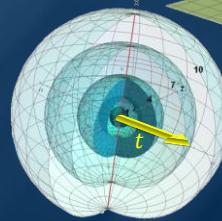
# Spacetime Foliations

Manifold foliation (*spacetime slicing*) is a covering space decomposition into hypersurfaces of lower dimension (e.g.,  $n-1$ ) paired with a smooth scalar field (regular with non-trivial gradient), so that each hypersurface (leaf) is a level surface of the scalar field.

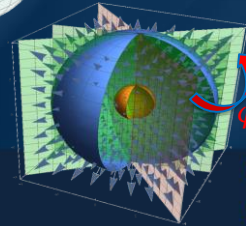
□ Space ( $x$ ) Foliation of Spacetime:



□ (Radial,  $t$ ) Time-Foliation of Spacetime:



□ (Angular,  $\varphi$ ) Phase-Foliation of Kime:



# Heisenberg's Uncertainty in Spacetime

- The classical Heisenberg 4D spacetime uncertainty may be explicated as a reduction of Einstein-like 5D deterministic dynamics. In other words, the common spacetime uncertainty principle could be understood as a consequence of deterministic laws in 5D spacetime.
- 4D Heisenberg uncertainty can be viewed as a silhouette of 5D Einstein deterministic dynamics. We can express the original Heisenberg's uncertainty relation between the momentum and the position using Einstein summation indexing convention:

$$\underbrace{dp^\mu}_{\text{increment in the 4-momentum}} \underbrace{dx_\mu}_{\text{increment in the 4-position}} \sim h.$$

We can divide both sides of this equation by two increments in the proper time  $s$ , which represents the time measured within the internal coordinate reference frame:

$$\frac{dp^\mu}{ds} \frac{dx_\mu}{ds} = F^\mu u_\mu \sim \frac{h}{ds^2}.$$

In the limit, this suggests that there is a force ( $F$ ) acting parallel to the velocity ( $u$ ), whose inner product with velocity is non-trivial. However, this contradicts the well-known orthogonality condition in Einstein's 4D theory of relativity.

- In 5D spacetime, the conventional geodesic motion is perturbed by an extra force  $f^\mu$  that can be decomposed into two parts  $f^\mu = f_\perp^\mu + f_\parallel^\mu$ , where  $f_\perp^\mu$  is normal to the 4-velocity and  $f_\parallel^\mu$  is parallel to the 4-velocity  $u^\mu$ . The normal component  $f_\perp^\mu$  is similar to other conventional forces and obeys the usual orthogonality condition  $f_\perp^\mu u_\mu = 0$ . However, the parallel component  $f_\parallel^\mu$  has no analog in 4D spacetime. In general, it has a non-trivial inner product with the 4-velocity  $u^\mu$ ,  $f_\parallel^\mu u_\mu \neq 0$ .

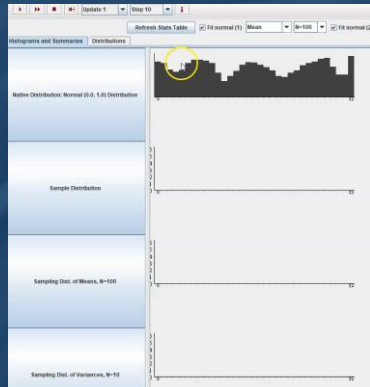
Wesson & Overduin (2018)

Dinov & Velez (2021)

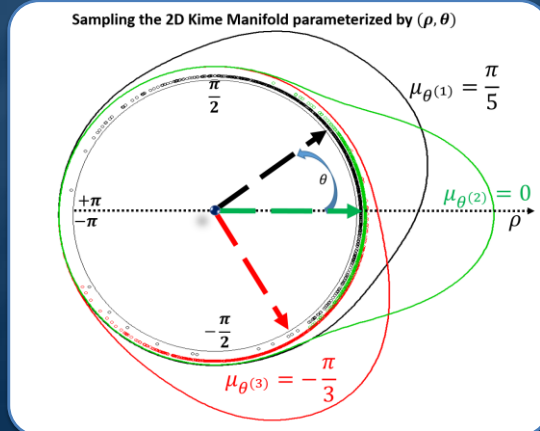


# Hidden Variable Theory & Random Sampling

- Kime phase distributions are mostly symmetric, random observations  $\equiv$  phase sampling



[http://wiki.stat.ucla.edu/socr/index.php/SOCR\\_EduMaterials\\_Activities\\_GeneralCentralLimitTheorem](http://wiki.stat.ucla.edu/socr/index.php/SOCR_EduMaterials_Activities_GeneralCentralLimitTheorem)

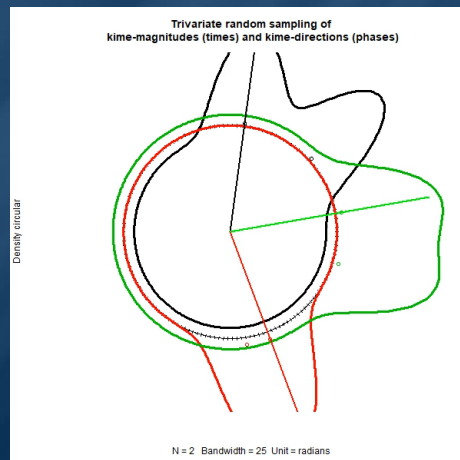


Dinov, Christou & Sanchez (2008)

Dinov & Velez (2021)



## Kime-Phase Sampling Simulation



<https://Spacekime.org>

Dinov & Velez (2021)



# Copenhagen vs. Spacekime Interpretations

## □ Copenhagen Interpretation

An instant measurement causes the wavefunction  $\Psi$  to randomly collapse only into one of the eigenfunctions of the quantity that is being measured.

$$\left\{ \begin{array}{l} \text{Probabilistic state of the system} \\ \Psi = \sum_{\alpha} c_{\alpha} \psi_{\alpha} \text{ (wavefunction)} \\ \text{Energy is unknown} \\ \text{Natural, intrinsic, fuzzy} \end{array} \right\} \xrightarrow[\text{observe the total energy}]{\text{Copenhagen Interpretation Measurement process}} \left\{ \begin{array}{l} \text{Wavefunction collapse} \\ \Psi = c_{\alpha_0} \psi_{\alpha_0}, \text{ for some index } \alpha_0, \\ c_{\alpha_0} \in \mathbb{C} \\ \text{Total Energy} = E_{\alpha_0} \\ \text{Instance of the observed state of the system} \end{array} \right.$$

## □ Spacekime Interpretations

$$\left\{ \begin{array}{l} \Psi(t) = \int_{-\pi}^{\pi} \Psi(t, \varphi) d\varphi \\ \text{Spacekime wavefunction} \\ \text{Unknown Total Energy} \\ \text{natural, intrinsic, fuzzy, probabilistic} \\ \text{state of the system} \end{array} \right\} \xrightarrow[\text{observe energy at time } t_0]{\text{Spacekime Interpretation Measurement process}} \left\{ \begin{array}{l} \Psi(t_0) = \Psi(t_0, \varphi'_0) \equiv \Psi(\varphi'_0) \left\{ \begin{array}{l} \text{wavefunction density} \\ \varphi'_0 \sim \Phi[-\pi, \pi] \left\{ \begin{array}{l} \text{kime - phase} \\ \text{distribution (symmetric)} \end{array} \right. \right. \\ \text{Observed Total Energy} = E_{\varphi'_0}, \text{ which} \\ \text{still represents an eigenvalue of the } \hat{H} \\ \text{observable state of the system} \end{array} \right.$$

For a fixed-time instantaneous measurement of the system at  $t = t_0$ , the wavefunction, or inference-function,  $\Psi(\alpha) = \Psi(t_0, \varphi)$  is naturally an aggregate measure over the entire kime-phase distribution with a range  $-\pi \leq \varphi < \pi$ . However, as the entire kime phases distribution ( $\Phi$ ) may not be directly, historically, and instantaneously observed, the actual measurement, or inference, only reflects a measurement  $\Psi(t_0, \varphi)$  for one random phase,  $\varphi_0$ . In other words, the natural state of the system is theoretically described by a wavefunction, or inference-function,

$$\Psi(t) = \int_{-\pi}^{\pi} \Psi(t, \varphi) d\varphi,$$

however, the actual observation reflects the value at a given time point ( $t_0$ ) for some fixed but randomly chosen phase,  $\varphi = \varphi_0$ . Thus, each observation manifests as an immutable instantaneous measurement value,  $\Psi(t_0) = \Psi(t_0, \varphi_0)$ . In a measure-theoretic sense, a pair of simultaneous ( $t = t_0$ ) independent measurements of the exact same spacekime system would naturally yield two distinct observed values.  $\Psi' \equiv \Psi(t_0, \varphi'_0)$  and  $\Psi'' \equiv \Psi(t_0, \varphi''_0)$ , where the two phases are independently sampled from the circular phase distribution, i.e.,  $\varphi_0, \varphi'_0 \sim \Phi[-\pi, \pi]$ .

Dinov & Velez (2021)



# Spacekime Open Math Problems

- Does kime have the same interpretation in quantum mechanics and in general relativity (relative to a specified origin), just like the spatial references? In other words, is kime universal and absolute?
- We know time, by itself, is excluded from the Wheeler-DeWitt equation. Is this true for kime as well? That is, does the Wheeler-DeWitt equation depend on kime the same way it depends on the particle location?
- Is there kime-dilation, reminiscent of time-dilation? In other words, does the action of moving objects affect (slow) kime? How?
- Explore the relations between various spacekime principles (e.g., space-kime motion and PDEs with respect to kime) and Painlevé equations in the complex plane.
- Extend the concepts of time-based evolution, time-varying processes, and probability to the 2D kime manifold.

Dinov & Velez (2021)



# Spacekime Open Math Problems

## □ Ergodicity

Let's look at the particle velocities in the 4D Minkowski spacetime  $(X)$ , a measure space where gas particles move spatially and evolve longitudinally in time. Let  $\mu = \mu_x$  be a measure on  $X$ ,  $f(x, t) \in L^1(X, \mu)$  be an integrable function (e.g., velocity of a particle), and  $T: X \rightarrow X$  be a measure-preserving transformation at position  $x \in \mathbb{R}^3$  at time  $t \in \mathbb{R}^+$ .

Prove a pointwise ergodic theorem arguing that in a measure theoretic sense, the average of  $f$  over all particles in the gas system at a fixed time,  $\bar{f} = E_t(f) = \int_{\mathbb{R}^3} f(x, t) d\mu_x$ , will be equal to the average velocity of just one particle over the entire time span,

$$\bar{f} = \lim_{n \rightarrow \infty} \left( \frac{1}{n} \sum_{i=0}^n f(T^i x) \right). \text{ That is, prove that } \bar{f} \equiv \hat{f}.$$

The spatial probability measure is denoted by  $\mu_x$  and the transformation  $T^i x$  represents the dynamics (time evolution) of the particle starting with an initial spatial location  $T^0 x = x$ . Investigate the ergodic properties of various transformations in the 5D Minkowski spacetime.

$$\bar{f} = E_t(f) = \int_{-\pi}^{+\pi} f(t, \phi) d\Phi \stackrel{?}{=} \lim_{t \rightarrow \infty} \left( \frac{1}{t} \sum_{i=0}^t f(t, \phi_0) \right) = \hat{f}$$

Dinov & Velez (2021)



# Spacekime Open Math Problems

## □ Inference Inner Product

Define the inner product between two inference functions,  $\langle \psi | \phi \rangle \equiv \langle \psi, \phi \rangle$ , as a measure of the level of inference overlap, result consistency, agreement or synergies between their corresponding inferential states. The inner product provides the foundation for a probabilistic interpretation of data science inference in terms of transition probabilities. The squared modulus of an inference function,  $\langle \psi | \psi \rangle = \|\psi\|^2$ , represents the probability density that allows us to measure specific inferential outcomes for a given set of observables. To facilitate probability interpretation, the law of total probability requires the normalization condition, i.e.,  $1 = \int \|\psi\|^2$ . Let's illustrate the modulus in the scope of logistic inference; the square modulus of the inference function is:

$$\begin{aligned} \|\psi\|^2 &= \langle \psi | \psi \rangle = \langle \psi(X, Y) | \psi(X, Y) \rangle = \langle \hat{\beta}^{OLS} | \hat{\beta}^{OLS} \rangle = \\ &= ((X^T X)^{-1} X^T Y | (X^T X)^{-1} X^T Y) = ((X^T X)^{-1} X^T Y)^T (X^T X)^{-1} X^T Y = \\ &= Y^T X (X^T X)^{-1} (X^T X)^{-1} X^T Y = Y^T \underbrace{X (X^T X)^{-2} X^T}_D Y = Y^T D Y = \left( \left( D^{\frac{1}{2}} \right)^T Y \right) \left( D^{\frac{1}{2}} Y \right) = \|Y\|_D^2. \end{aligned}$$

What would be the effect of exploring the use of the matrix  $D$  as a constant normalization factor  $(D^{\frac{1}{2}})$ ? Define an appropriate **coherence metric** that captures the agreement, or overlap, between a pair of complementary inference functions or data analytic strategies. E.g., inference consistency measures may be based on:

$$\text{Coherence} = \frac{\langle \psi | \phi \rangle}{\sqrt{\langle \psi | \psi \rangle \times \langle \phi | \phi \rangle}} = \frac{\langle \psi | \phi \rangle}{\|\psi\| \|\phi\|}.$$

Alternatively, as the data represent random variables (vectors, or tensors) and the specific data-analytic strategy yields the inference function, explore **mutual information of operators**, i.e., linear or non-linear operator acting on the data:

$$I(\psi; \phi) = \sum_i \sum_j \langle \psi_i | \phi_j \rangle \log \left( \frac{\langle \psi_i | \phi_j \rangle}{\|\psi_i\| \|\phi_j\|} \right),$$

where the inference states  $\psi_i$  and  $\phi_i$  are eigenfunctions corresponding to some eigenvalues  $O_i$ .

Dinov & Velez (2021)





# Spacekime Connection to Data Analytics?



## Mathematical-Physics $\Rightarrow$ Data Science

Mathematical-Physics	Data Science
A <b>particle</b> is a small localized object that permits observations and characterization of its physical or chemical properties	An <b>object</b> is something that exists by itself, actually or potentially, concretely or abstractly, physically or incorporeal (e.g., person, subject, etc.)
An <b>observable</b> a dynamic variable about particles that can be measured	A <b>feature</b> is a dynamic variable or an attribute about an object that can be measured
Particle <b>state</b> is an observable particle characteristic (e.g., position, momentum)	<b>Datum</b> is an observed quantitative or qualitative value, an instantiation, of a feature
Particle <b>system</b> is a collection of independent particles and observable characteristics, in a closed system	<b>Problem</b> , aka Data System, is a collection of independent objects and features, without necessarily being associated with apriori hypotheses
<b>Wave-function</b>	<b>Inference-function</b>
Reference-Frame <b>transforms</b> (e.g., Lorentz)	Data <b>transformations</b> (e.g., wrangling, log-transform)
<b>State of a system</b> is an observed measurement of all particles ~ wavefunction	<b>Dataset (data)</b> is an observed instance of a set of datum elements about the problem system, $O = \{X, Y\}$
A <b>particle system is computable</b> if (1) the entire system is logical, consistent, complete and (2) the unknown internal states of the system don't influence the computation (wavefunction, intervals, probabilities, etc.)	<b>Computable data object</b> is a very special representation of a dataset which allows direct application of computational processing, modeling, analytics, or inference based on the observed dataset
...	...



# Mathematical-Physics $\Rightarrow$ Data Science

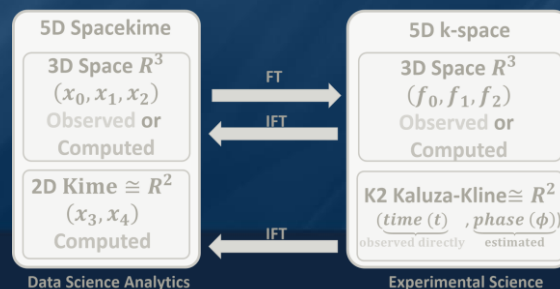
Math-Physics	Data Science
<p><u>Wavefunction</u></p> <p>Wave equ problem:</p> $\left(\frac{\partial^2}{\partial x^2} - \frac{1}{v^2} \frac{\partial^2}{\partial t^2}\right) \psi(x, t) = 0$ <p>Complex Solution:</p> $\psi(x, t) = A e^{i(kx - \omega t)}$ <p>where <math>\left \frac{\omega}{k}\right  = v</math>,</p> <p>represents a traveling wave</p>	<p><u>Inference function</u> - describing a solution to a specific data analytic system (a problem). For example,</p> <ul style="list-style-type: none"> <li>A <u>linear (GLM) model</u> represents a solution of a prediction inference problem, <math>Y = X\beta</math>, where the inference function quantifies the effects of all independent features (<math>X</math>) on the dependent outcome (<math>Y</math>), data: <math>O = \{X, Y\}</math>:  <math display="block">\psi(O) = \psi(X, Y) \Rightarrow \hat{\beta} = \hat{\beta}^{OLS} = (X X)^{-1} \langle X Y \rangle = (X^T X)^{-1} X^T Y.</math></li> <li>A non-parametric, <u>non-linear</u>, alternative inference is SVM classification. If <math>\psi_x \in H</math>, is the lifting function <math>\psi: R^\eta \rightarrow R^d</math> (<math>\psi: x \in R^\eta \rightarrow \tilde{x} = \psi_x \in H</math>), where <math>\eta \ll d</math>, the kernel <math>\psi_x(y) = \langle x y \rangle: O \times O \rightarrow R</math> transforms non-linear to linear separation, the observed data <math>O_i = \{x_i, y_i\} \in R^\eta</math> are lifted to <math>\psi_{O_i} \in H</math>. Then, the SVM prediction operator is the weighted sum of the kernel functions at <math>\psi_{O_i}</math>, where <math>\beta^*</math> is a solution to the SVM regularized optimization:  <math display="block">\langle \psi_O   \beta^* \rangle_H = \sum_{i=1}^n p_i^* \langle \psi_O   \psi_{O_i} \rangle_H</math></li> </ul> <p>The linear coefficients, <math>p_i^*</math>, are the dual weights that are multiplied by the label corresponding to each training instance, <math>\{y_i\}</math>.</p> <p>Inference always depends on the (input) data; however, it does not have 1-1 and onto bijective correspondence with the data, since the inference function quantifies predictions in a probabilistic sense.</p>

GLM/SVM: <http://DSPA.predictive.space> | Dinov, Springer (2018)



## Spacetime Analytics


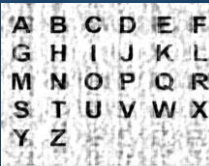
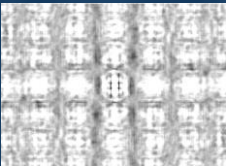
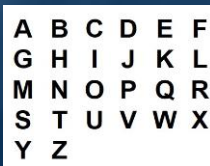


- Let's assume that we have:
  - (1) Kime extension of Time, and
  - (2) Parallels between wavefunctions  $\leftrightarrow$  inference functions
- Often, we can't directly observe (record) data natively in 5D spacetime.
- Yet, we can measure quite accurately the kime-magnitudes ( $r$ ) as event orders, "times".
- To reconstruct the 2D spatial structure of kime, borrow tricks used by crystallographers<sup>1</sup> to resolve the structure of atomic particles by only observing the magnitudes of the diffraction pattern in k-space. This approach heavily relies on (1) prior information about the kime directional orientation (that may be obtained from using similar datasets and phase-aggregator analytical strategies), or (2) experimental reproducibility by repeated confirmations of the data analytic results using longitudinal datasets.



<sup>1</sup> Rodriguez, Ivanova, Nature 2015



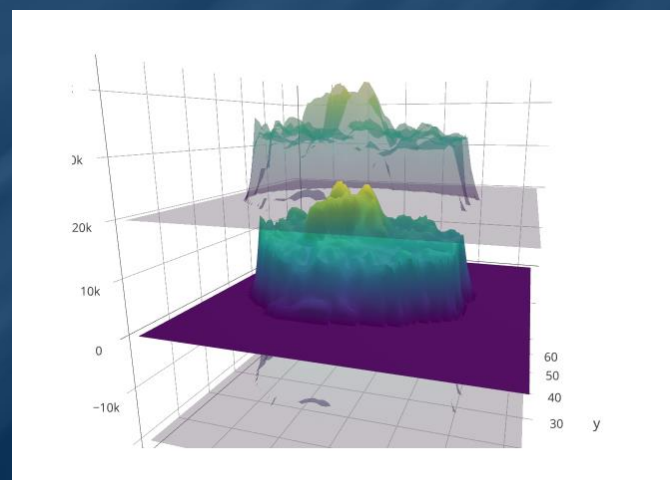
## 2D Image Analysis / Character Recognition

		Kime-direction (Phase) Synthesis			Observed Data
		Correct Phase	Swapped Phase	Nil-Phase	
2D Images	Cyrillic Alphabet				
	English Alphabet				

Dinov &amp; Velez (2021)



## Back to fMRI (4D spacetime data)

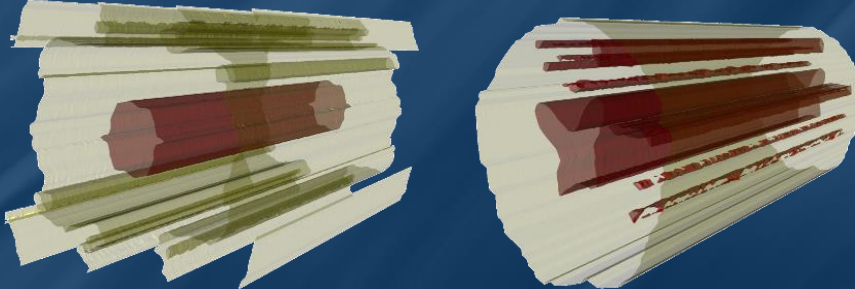


3D rendering of 3 time cross-sections of the fMRI series over a 2D spatial domain



## Spacekime Analytics: fMRI Example

- 3D isosurface Reconstruction of (space=2, time=1) fMRI signal



**4D spacetime:** Reconstruction using trivial phase-angle; kime=time=(magnitude, 0)

**5D Spacekime:** Reconstruction using correct kime=(magnitude, phase)

3D pseudo-spacetime reconstruction:

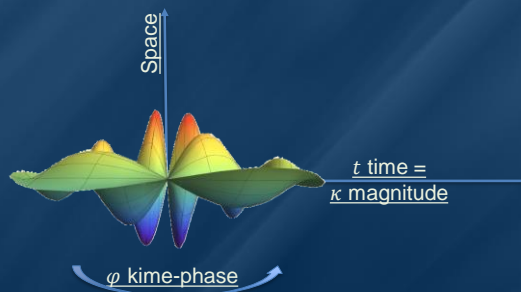
$$f = \hat{h} \left( \underbrace{x_1, x_2}_{\text{space}}, \underbrace{t}_{\text{time}} \right)$$



## Spacekime Analytics: Kime-series = Surfaces (not curves)

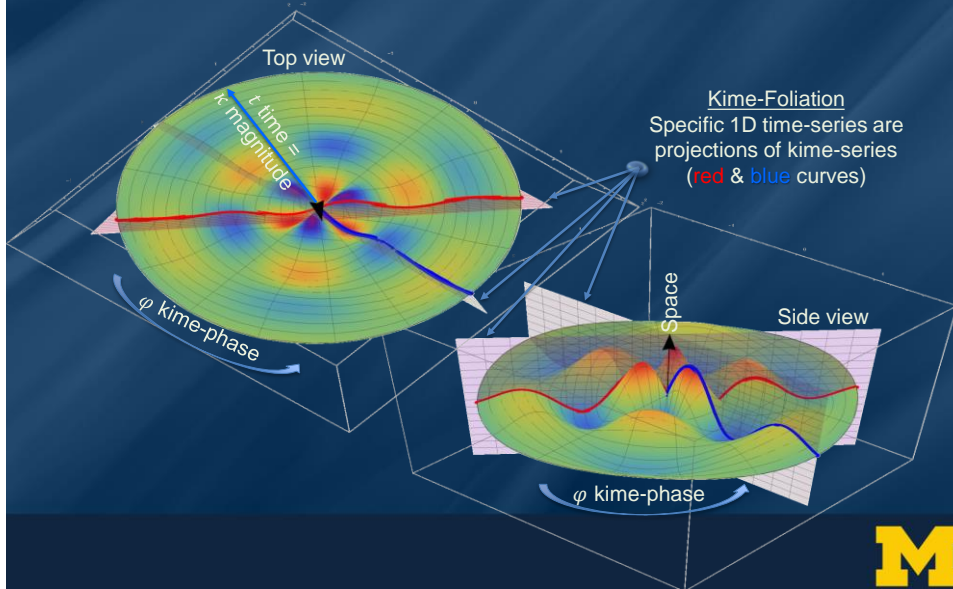
In the 5D spacekime manifold, time-series curves extend to kime-series, i.e., surfaces parameterized by kime-magnitude ( $t$ ) and the kime-phase ( $\varphi$ ).

Kime-phase aggregating operators that can be used to transform standard time-series curves to spacekime kime-surfaces, which can be modeled, interpreted, and predicted using advanced spacekime analytics.



## Spacekime Analytics: fMRI kime-series

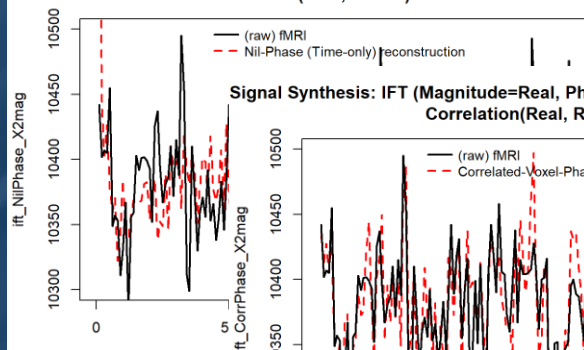
fMRI kime-series at a single spatial voxel location (rainbow color represents fMRI kime intensities)



## Spacekime Analytics: fMRI Example

Reconstruction of the fMRI timeseries at a single spatial voxel location

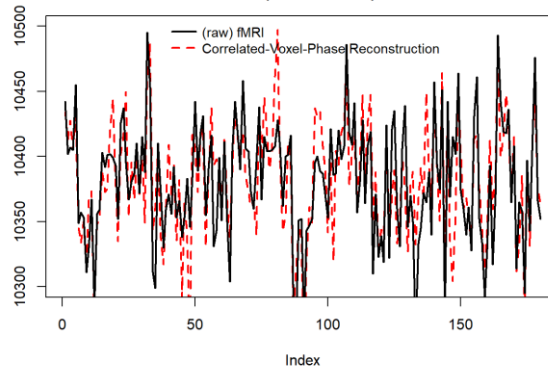
**Signal Synthesis: IFT (Magnitude=Real, Phase=Nil)**  
 Correlation(Real, Recon) = 0.157



Cor(Orig, Nil-Phase) = 0.16

Cor(Orig, Estim-Phase) = 0.79

**Signal Synthesis: IFT (Magnitude=Real, Phase=Highly-Correlated (0.702) V)**  
 Correlation(Real, Recon) = 0.789



# Statistical Implications of Spacekime Analytics



## Uncertainty

- Quantum Mechanics:  $\|D_x u\| \|xu\| = \langle \frac{\hbar}{i} \partial_x u | i x u \rangle = \frac{\hbar}{2} \|u\|^2 > 0$ , i.e., non-commutation of the unbounded operators  $D_x = \frac{\hbar}{i} \partial_x$  and  $x$ , (multiplication by  $x$ ).
- Signal processing: Functions can't be time-limited **and** band-limited. Alternatively, a function and its Fourier transform cannot both have bounded domains  $\sigma_t \times \sigma_\omega \geq 1/(4\pi)$ , where  $\sigma_t, \sigma_\omega$  are the time and frequency SDs.
- Entropic uncertainty: Entropy can be used just like the SD to quantify distribution structure. For instance, for angular, bimodal, or divergent-variance distributions, Entropy may be a better measure of dispersion than SD. For  $FT(f)(\omega) = \hat{f}(\omega)$  and  $IFT(\hat{f})(x) = \hat{\hat{f}}(x)$ , the Shannon information entropies:
 
$$H_x = \int \hat{f}(x) \log(\hat{f}(x)) dx \text{ and } H_\omega = \int \hat{f}(\omega) \log(\hat{f}(\omega)) d\omega .$$
 satisfy:  $H_x + H_\omega \geq \log(e/2)$ .
- $L^2(\mathbb{R})$  uncertainty: it is impossible for  $f \in L^2$  and  $\hat{f}$  to both decrease extremely rapidly. If both have rapidly decreasing tails:  $|f(x)| \leq C(1 + |x|)^n e^{-a\pi x^2}$  and  $|\hat{f}(\omega)| \leq C(1 + |\omega|)^n e^{-b\pi \omega^2}$ , for some constant  $C$ , polynomial power  $n$ , and  $a, b \in \mathbb{R}$ , then  $f = 0$  (when  $ab > 1$ );  $f(x) = P_k(x)e^{-a\pi x^2}$  and  $\hat{f}(\omega) = \widehat{P_k}(\omega) * e^{-\omega^2/4\pi a}$ , where  $\deg(P_k) \leq n$  (when  $ab = 1$ ); or (when  $ab < 1$ ).





## Heisenberg's Uncertainty in Spacekime?

- ❑ Heisenberg's uncertainty is resolved in 5D spacekime
- ❑ We can derive the classical 4D spacetime Heisenberg uncertainty as a reduction of Einstein-like 5D deterministic dynamics:
  - ❑ The math is terse – it involves deriving the equations of motion by maximizing the distance (integral along the geodesic) between two points in 5D spacekime
  - ❑ The inner product  $du^\mu dx_\mu = \frac{dx^\mu dx_\mu}{L} = \frac{ds^2}{L}$ . Since  $\frac{ds}{L} \rightarrow 1$  near the leaf membrane,  $du^\mu dx_\mu = L = \frac{h}{mc}$ . Replacing the change in velocity ( $du^\mu$ ) by the change in momentum ( $dp^\mu$ ) yields:  $dp^\mu dx_\mu = h$ .
  - ❑ This relation is similar to the quantum mechanics uncertainty principle in 4D Minkowski spacetime; however, it is obtained from 5D Einstein deterministic dynamics. In other words, in spacetime, Heisenberg's uncertainty principle manifests simply because of the one degree of freedom (kime-phase), i.e., lack of sufficient information about the second kime dimension.
  - ❑ In 5D spacekime, the conventional geodesic motion is perturbed by an extra force  $f^\mu$  that can be split into two parts  $f^\mu = f_{\perp}^\mu + f_{\parallel}^\mu$ . The normal component  $f_{\perp}^\mu$  is similar to other conventional forces and obeys the usual orthogonality condition  $f_{\perp}^\mu u_\mu = 0$ . However, the parallel component  $f_{\parallel}^\mu$  has no analog in 4D spacetime. In general, it has a non-trivial inner product with the 4-velocity  $u^\mu$ ,  $f_{\parallel}^\mu u_\mu \neq 0$ .
- ❑ In Minkowski 4D spacetime, the lack of kime-phase data naturally leaves one degree of freedom in the system causing Heisenberg's uncertainty. However, the latter can be explicated by information knowledge of the fifth component (kime-phase).

Wesson & Overduin, World Scientific (2018) | Dinov & Veleev (2021)



## Bayesian Inference Representation

- ❑ Suppose we have a single spacetime observation  $X = \{x_{i_o}\} \sim p(x | \gamma)$  and  $\gamma \sim p(\gamma | \varphi = \text{phase})$  is a process parameter (or vector) that we are trying to estimate.
- ❑ Spacekime analytics aims to make appropriate inference about the process  $X$ .
- ❑ The sampling distribution,  $p(x | \gamma)$ , is the distribution of the observed data  $X$  conditional on the parameter  $\gamma$  and the prior distribution,  $p(\gamma | \varphi)$ , of the parameter  $\gamma$  before the data  $X$  is observed,  $\varphi = \text{phase aggregator}$ .
- ❑ Assume that the hyperparameter (vector)  $\varphi$ , which represents the kime-phase estimates for the process, can be estimated by  $\hat{\varphi} = \varphi'$ .
- ❑ Such estimates may be obtained from an oracle, approximated using similar datasets, acquired as phases from samples of analogous processes, or derived via some phase-aggregation strategy.
- ❑ Let the posterior distribution of the parameter  $\gamma$  given the observed data  $X = \{x_{i_o}\}$  be  $p(\gamma | X, \varphi')$  and the process parameter distribution of the kime-phase hyperparameter vector  $\varphi$  be  $\gamma \sim p(\gamma | \varphi)$ .



# Bayesian Inference Representation

- We can formulate spacekime inference as a Bayesian parameter estimation problem:

$$\begin{aligned} \underbrace{\frac{p(\gamma|X, \varphi')}{\text{posterior distribution}}}_{\text{posterior distribution}} &= \frac{p(\gamma, X, \varphi')}{p(X, \varphi')} = \frac{p(X|\gamma, \varphi') \times p(\gamma, \varphi')}{p(X, \varphi')} = \frac{p(X|\gamma, \varphi') \times p(\gamma, \varphi')}{p(X|\varphi') \times p(\varphi')} = \\ &= \frac{p(X|\gamma, \varphi')}{p(X|\varphi')} \times \frac{p(\gamma, \varphi')}{p(\varphi')} = \frac{p(X|\gamma, \varphi') \times p(\gamma|\varphi')}{\underbrace{p(X|\varphi')}_{\text{observed evidence}}} \propto \underbrace{\frac{p(X|\gamma, \varphi')}{\text{likelihood}}}_{\text{likelihood}} \times \underbrace{\frac{p(\gamma|\varphi')}{\text{prior}}}_{\text{prior}}. \end{aligned}$$

- In Bayesian terms, the posterior probability distribution of the unknown parameter  $\gamma$  is proportional to the product of the likelihood and the prior.
- In probability terms, the posterior = likelihood times prior, divided by the observed evidence, in this case, a single spacetime data point,  $x_{i_o}$ .



# Bayesian Inference Representation

- Spacekime analytics based on a single spacetime observation  $x_{i_o}$  can be thought of as a type of Bayesian prior-predictive or posterior-predictive distribution estimation problem.

- Prior predictive distribution of a new data point  $x_{j_o}$ , marginalized over the *prior* – i.e., the sampling distribution  $p(x_{j_o}|\gamma)$  weight-averaged by the pure *prior* distribution):

$$p(x_{j_o}|\varphi') = \int p(x_{j_o}|\gamma) \times \underbrace{p(\gamma|\varphi')}_{\text{prior distribution}} d\gamma.$$

- Posterior predictive distribution of a new data point  $x_{j_o}$ , marginalized over the *posterior*; i.e., the sampling distribution  $p(x_{j_o}|\gamma)$  weight-averaged by the *posterior* distribution:

$$p(x_{j_o}|x_{i_o}, \varphi') = \int p(x_{j_o}|\gamma) \times \underbrace{p(\gamma|x_{i_o}, \varphi')}_{\text{posterior distribution}} d\gamma.$$

- The difference between these two predictive distributions is that
  - the posterior predictive distribution is updated by the observation  $X = \{x_{i_o}\}$  and the hyperparameter,  $\varphi$  (phase aggregator),
  - whereas the prior predictive distribution only relies on the values of the hyperparameters that appear in the prior distribution.



## Bayesian Inference Representation

- ❑ The posterior predictive distribution may be used to sample or forecast the distribution of a prospective, yet unobserved, data point  $x_{j_o}$ .
- ❑ The posterior predictive distribution spans the entire parameter state-space ( $\text{Domain}(\gamma)$ ), just like the wavefunction represents the distribution of particle positions over the complete particle state-space.
- ❑ Using maximum likelihood or maximum *a posteriori* estimation, we can also estimate an individual parameter point-estimate,  $\gamma_o$ . In this frequentist approach, the point estimate may be plugged into the formula for the distribution of a data point,  $p(x | \gamma_o)$ , which enables drawing IID samples or individual outcome values.



## Bayesian Inference Simulation

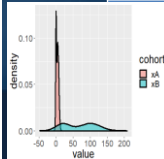
- ❑ Simulation example using 2 random samples drawn from mixture distributions each of  $n_A = n_B = 10K$  observations:
  - ❑  $\{X_{A,i}\}_{i=1}^{n_A}$ , where  $X_{A,i} = 0.3U_i + 0.7V_i$ ,  $U_i \sim N(0,1)$  and  $V_i \sim N(5,3)$ , and
  - ❑  $\{X_{B,i}\}_{i=1}^{n_B}$ , where  $X_{B,i} = 0.4P_i + 0.6Q_i$ ,  $P_i \sim N(20,20)$  and  $Q_i \sim N(100,30)$ .
- ❑ The intensities of cohorts  $A$  and  $B$  are independent and follow different mixture distributions. We'll split the first cohort ( $A$ ) into training ( $C$ ) and testing ( $D$ ) subgroups, and then:
  - ❑ Transform all four cohorts into Fourier k-space,
  - ❑ Iteratively randomly sample single observations from (training) cohort  $C$ ,
  - ❑ Reconstruct the data into spacetime using a single kime-magnitude value and alternative kime-phase estimates derived from cohorts  $B$ ,  $C$ , and  $D$ , and
  - ❑ Compute the classical spacetime-derived population characteristics of cohort  $A$  and compare them to their spacekime counterparts obtained using a single  $C$  kime-magnitude paired with  $B$ ,  $C$ , or  $D$  kime-phases.



# Bayesian Inference Simulation

Summary statistics for the original process (cohort *A*) and the corresponding values of their counterparts computed using the spacekime reconstructed signals based on kime-phases of cohorts *B*, *C*, and *D*. The estimates for the latter three cohorts correspond to reconstructions using a single spacetime observation (i.e., single kime-magnitude) and alternative kime-phases (in this case, kime-phases derived from cohorts *B*, *C*, and *D*).

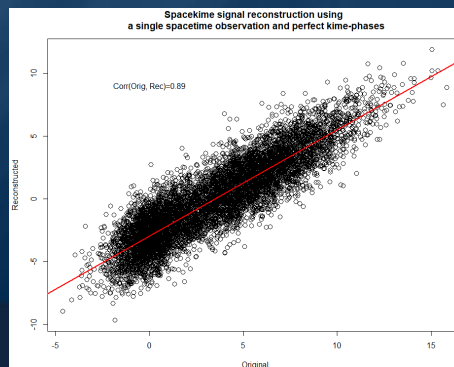
	Spacetime	Spacekime Reconstructions (single kime-magnitude)		
Summaries	(A)	(B)	(C)	(D)
	Original	Phase=Diff. Process	Phase=True	Phase=Independent
Min	-2.38798	-3.798440	-2.98116	-2.69808
1 <sup>st</sup> Quartile	-0.89359	-0.636799	-0.76765	-0.76453
Median	0.03311	0.009279	-0.05982	-0.08329
Mean	0.00000	0.000000	0.00000	0.00000
3 <sup>rd</sup> Quartile	0.75772	0.645119	0.72795	0.69889
Max	3.61346	3.986702	3.64800	3.22987
Skewness	0.348269	0.001021943	0.2372526	0.31398
Kurtosis	-0.68176	0.2149918	-0.4452207	-0.3270084



# Bayesian Inference Simulation

The correlation between the original data (*A*) and its reconstruction using a single kime magnitude and the correct kime-phases (*C*) is  $\rho(A, C) = 0.89$ .

This strong correlation suggests that a substantial part of the *A* process energy can be recovered using only a single observation. In this case, to reconstruct the signal back into spacetime and compute the corresponding correlation, we used a single kime-magnitude (sample-size=1) and process *C* kime-phases.



# Bayesian Inference Simulation

Let's demonstrate the Bayesian inference corresponding to this spacekime data analytic problem using a simulated bimodal experiment:

$$X_A = 0.3U + 0.7V, \text{ where } U \sim N(0,1) \text{ and } V \sim N(5,3)$$

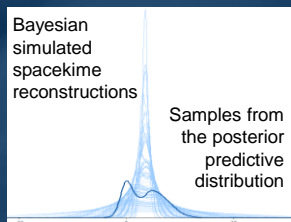
Specifically, we will illustrate the Bayesian inference using repeated single spacetime observations from cohort  $A$ ,  $X = \{x_{i_0}\}$ , and varying kime-phase priors ( $\theta$  = phase aggregator) obtained from cohorts  $B$ ,  $C$ , or  $D$ , using different posterior predictive distributions

Relations between the empirical data distribution (**dark blue**) and samples from the posterior predictive distribution, representing Bayesian simulated spacekime reconstructions (**light-blue**). The derived Bayesian estimates do not perfectly match the empirical distribution of the simulated data, yet there is clearly information encoding that is captured by the spacekime data reconstructions

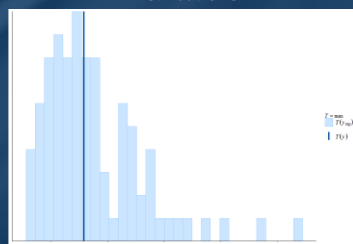
This signal compression can be exploited by subsequent model-based or model-free data analytic strategies for retrospective prediction, prospective forecasting, ML classification, derived clustering, and other spacekime inference methods



# Bayesian Inference Simulation

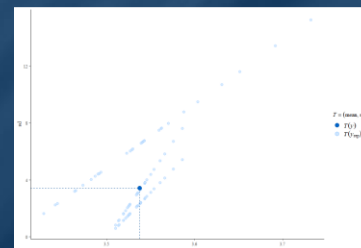


Distributions

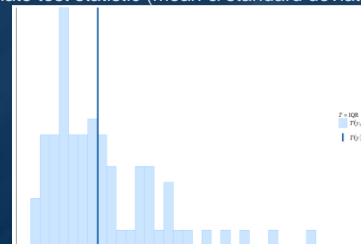


Test statistic (maximum)

Relations between the empirical data distribution (**dark blue**) and samples from the posterior predictive distribution, Bayesian simulated spacekime reconstructions (**light-blue**).



Bivariate test statistic (mean & standard deviation)



Test statistic (inter-quartile range, IQR)

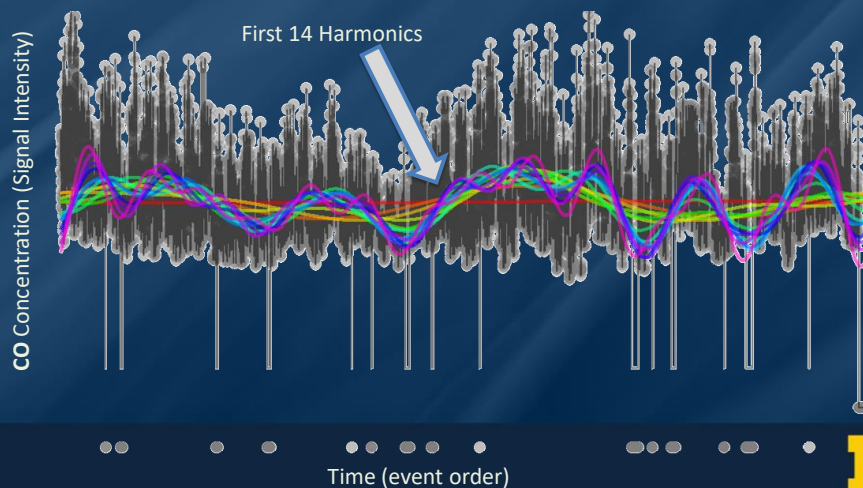


# Applications – Longitudinal Spacekime Data Analytics



## Exogenous Feature Time-series Analysis

ARIMAX modeling of UCI ML Air Quality Dataset (9,358 hourly-averaged CO responses from an array of sensors). Demonstrate the effect of kime-direction on the analysis of the longitudinal data.





# Exogenous Feature Time-series Analysis

CO ARIMAX models derived on 3 different  
signal reconstructions based on alternative  
kime-direction estimates

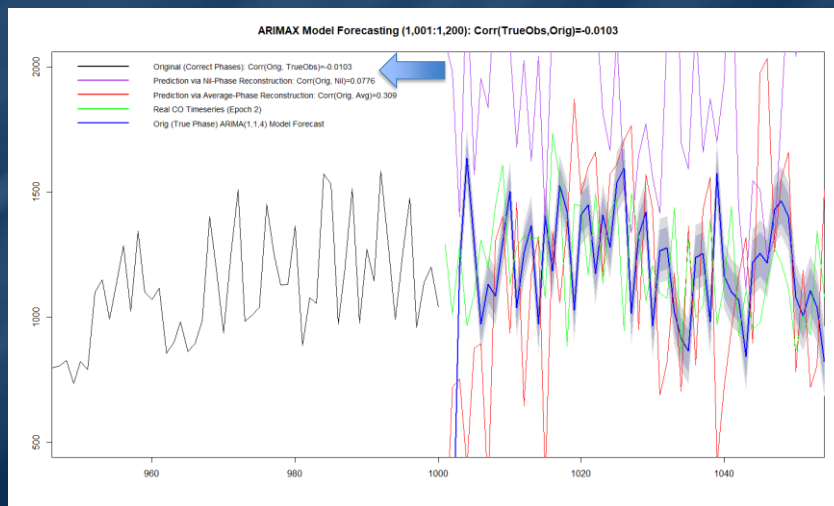
Phase	Nil	Average	True=original
Model Estimate	ARIMA(2,0,1)	ARIMA(2,0,3)	ARIMA(1,1,4)
AIC	<b>13179</b>	<b>14183</b>	<b>10581</b>
ar1	<b>1.11406562</b>	<b>0.329482302</b>	<b>0.2765312</b>
ar2	-0.14565048	0.238363531	.
ma1	-0.78919188	0.267291585	-0.88913497
ma2	.	<b>-0.006079386</b>	<b>0.12679494</b>
ma3	.	<b>0.15726556</b>	<b>0.03043726</b>
ma4	.	.	-0.17655728
intercept	503.3455144	742.800113	.
xreg1	-0.40283891	0.58379483	0.08035744
xreg2	<b>0.13656613</b>	<b>0.280936931</b>	<b>6.14947902</b>
xreg3	-0.51457636	-0.649722755	0.09859223
xreg4	1.09611981	1.239910298	0.01634736
xreg5	<b>1.21946209</b>	<b>-0.026110332</b>	<b>-0.04816591</b>
xreg6	<b>1.30628469</b>	<b>1.081777956</b>	<b>-0.01104142</b>
xreg7	<b>1.20868397</b>	<b>0.254018471</b>	<b>0.1832854</b>
xreg8	<b>1.14905809</b>	<b>0.306524131</b>	<b>0.17648482</b>
xreg9	<b>-0.48233756</b>	<b>-0.405204908</b>	<b>6.53739782</b>
xreg10	<b>0.03145281</b>	<b>0.351063312</b>	<b>1.79388326</b>
xreg11	-0.46395772	-0.457689796	-12.06965578

**ARIMAX (p,d,q)**  
p = order (# of time lags) of the AR part  
d = differencing (# of past values subtractions)  
q = order of MA part

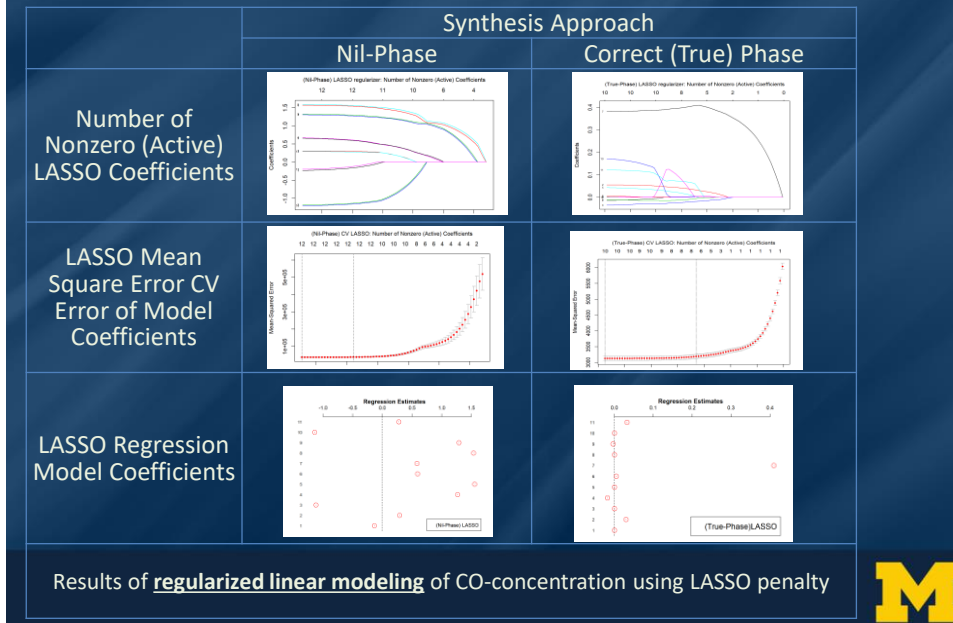


## Exogenous Feature Timeseries Forecasting

CO ARIMAX models derived on 3 different  
signal reconstructions based on alternative  
kime-direction estimates

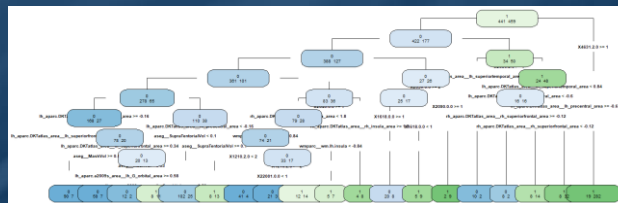


# Exogenous Feature Time-series Analysis



## Big Data Analytics Study – UKBB

- 9,914 UKBB participants; 7,614 features:  
Features: clinical+phenotypic variables (5K) and derived neuroimaging biomarkers (2.5K)
- Supervised Decision Tree (binary Dx) Classification – Correct Kime-Phase Estimates

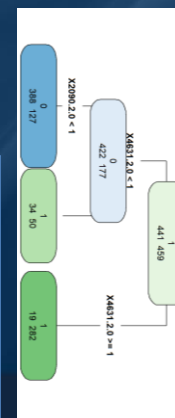


### Raw Decision Tree

```
## Prediction 0 1
##      0 362 60
##      1 79 399
## Accuracy: 0.8456
## 95% CI : (0.82, 0.87)
## No Information Rate: 0.51
## P-Value [Acc > NIR] : <2e-16
## Kappa: 0.6907
## McNemar's Test P-Value: 0.1268
## Sensitivity: 0.8209
## Specificity: 0.8693
## Detection Rate: 0.4022
## Detection Prevalence: 0.4689
## Balanced Accuracy: 0.8451
```

### Pruned Decision Tree

```
## Prediction 0 1
##      0 388 127
##      1 53 332
## Accuracy: 0.8
## 95% CI : (0.77, 0.83)
## No Information Rate: 0.51
## P-Value [Acc > NIR] : < 2.2e-16
## Kappa: 0.6012
## McNemar's Test P-Value: 5.295e-08
## Sensitivity: 0.8798
## Specificity: 0.7233
## Detection Prevalence: 0.5722
## Balanced Accuracy: 0.8016
```

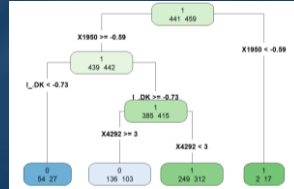


Zhou, et al. SREP (2019)



# Big Data Analytics Study – UKBB

- 9,914 UKBB participants (11 epochs of 900 cases); 7,614 clinical measurements, phenotypic features, and derived neuroimaging biomarkers Supervised Decision Tree (binary) Classification – **Epoch-average Kime-Phases**



**Raw Decision Tree**

```
## Reference
## Prediction 0 1
## 0 354 85
## 1 87 374
## Accuracy : 0.8089
## 95% CI : (0.78, 0.83)
## No Information Rate : 0.51
## P-Value [Acc > NIR] : <2e-16
## Kappa : 0.6176
## McNemar's Test P-Value : 0.9392
## Sensitivity : 0.8027
## Specificity : 0.8148
## Detection Rate : 0.3933
## Detection Prevalence : 0.4878
## Balanced Accuracy : 0.8088
```

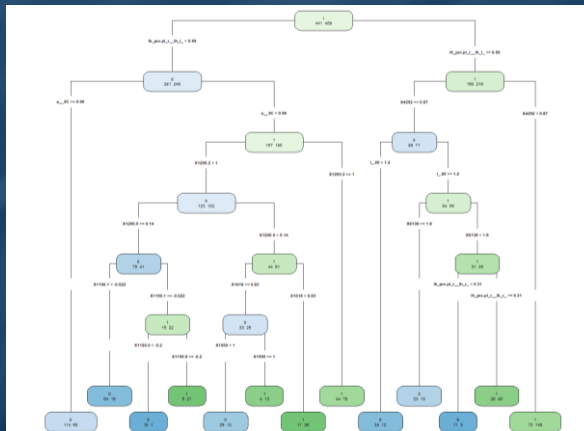
**Pruned Decision Tree**

```
## Reference
## Prediction 0 1
## 0 190 130
## 1 251 329
## Accuracy : 0.5767
## 95% CI : (0.54, 0.61)
## No Information Rate : 0.51
## P-Value [Acc > NIR] : 3.501e-05
## Kappa : 0.1484
## McNemar's Test P-Value : 7.857e-10
## Sensitivity : 0.4308
## Specificity : 0.7168
## Detection Rate : 0.2111
## Detection Prevalence : 0.3556
## Balanced Accuracy : 0.5738
```



# Big Data Analytics Study – UKBB

- 9,914 UKBB participants; 7,614 clinical measurements, phenotypic features, and derived neuroimaging biomarkers
- Supervised Decision Tree (binary) Classification – **Nil-average Kime-Phases**



**Raw Decision Tree**

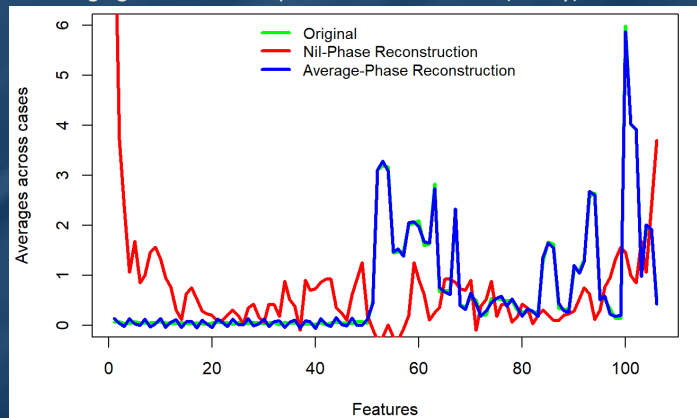
```
## Reference
## Prediction 0 1
## 0 341 86
## 1 100 373
## Accuracy : 0.7933
## 95% CI : (0.77, 0.82)
## No Information Rate : 0.51
## P-Value [Acc > NIR] : <2e-16
## Kappa : 0.5862
## McNemar's Test P-Value : 0.3405
## Sensitivity : 0.7732
## Specificity : 0.8126
## Detection Rate : 0.3789
## Detection Prevalence : 0.4744
## Balanced Accuracy : 0.7929
```

Pruned Decision Tree (not shown) was degenerate



# Big Data Analytics Study – UKBB

- 9,914 UKBB participants; 7,614 clinical measurements, phenotypic features, and derived neuroimaging biomarkers. Supervised Decision Tree (binary) Classification

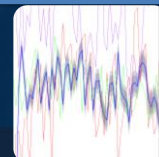
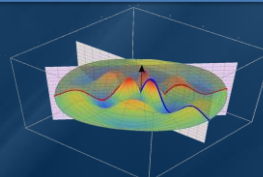
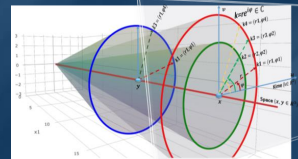


Overall feature averages across cases for the 3 complementary time-reconstruction analytic strategies



## Summary

- Need new methods to tackle important Big Biomed/Health Data Challenges
- Spacekime* representation makes a difference in predictive analytics
- Math models useful for representation & analysis of complex-temporal data
- Spacekime transform* enables small sample inference
- Optimal *kime-phase* aggregators?
- Spacekime* analytics representation has lots of “Open problems” (math, stats, DS)



# Interested in Spacekime Analytics?

- ☐ Check [www.SpaceKime.org](http://www.SpaceKime.org)
- ☐ Contact me
- ☐ We have lots of “Open Problems”



## Acknowledgments

Slides Online:  
“SOCR News”

### Funding

NIH: P20 NR015331, U54 EB020406, P50 NS091856, P30 DK089503, UL1TR002240, R01CA233487  
NSF: 1916425, 1734853, 1636840, 1416953, 0716055, 1023115

### Collaborators

- ☐ **SOCR:** Milen Velez, Yongkai Qiu, Zhe Yin, Yufei Yang, Daxuan Deng, Yueyang Shen, Alexandr Kalinin, Selvam Palanimalai, Syed Husain, Matt Leventhal, Ashwini Khare, Rami Elkest, Abhishek Chowdhury, Patrick Tan, Pratyush Pati, Brian Zhang, Juana Sanchez, Dennis Pearl, Kyle Siegrist, Rob Gould, Nicolas Christou, Hanbo Sun, Tuo Wang, Yi Wang, Lu Wei, Lu Wang, Simeone Marino
- ☐ **LONI/NI:** Arthur Toga, Roger Woods, Jack Van Horn, Zhuowen Tu, Yonggang Shi, David Shattuck, Elizabeth Sowell, Katherine Narr, Anand Joshi, Shantanu Joshi, Paul Thompson, Luminita Vese, Stan Osher, Stefano Soatto, Seok Moon, Junning Li, Young Sung, Carl Kesselman, Fabio Macciardi, Federica Torri
- ☐ **UMich MIDAS/MNORC/AD/PD Centers:** Cathie Spino, Chuck Burant, Ben Hampstead, Kayvan Najarian, Stephen Goutman, Stephen Strobbe, Hiroko Dodge, Bill Dauer, Chris Monk, Issam El Naqa, HV Jagadish, Brian Athey



<http://SOCR.umich.edu>